Available online at www.sciencedirect.com
SCIENCE DIRECT
Advances in Water Resources 29 (2006) 899–911
Advances in Water Resources
www.elsevier.com/locate/advwatres

A comparative study of Monte Carlo simple genetic algorithm and noisy genetic algorithm for cost-effective sampling network design under uncertainty

Jianfeng Wu [a,b], Chunmiao Zheng [b,*], Calvin C. Chien [c], Li Zheng [d]

[a] Department of Earth Sciences, Nanjing University, Nanjing 210093, China
[b] Department of Geological Sciences, 202 Bevill Research Building, University of Alabama, Tuscaloosa, AL 35487, United States
[c] Corporate Remediation, DuPont Company, Wilmington, DE 19805, United States
[d] Agricultural Resources Research Center, IGDB, Chinese Academy of Sciences, Shijiazhuang 050021, China

Received 10 December 2004; received in revised form 12 August 2005; accepted 17 August 2005
Available online 11 October 2005

Abstract

This study evaluates and compares two methodologies, Monte Carlo simple genetic algorithm (MCSGA) and noisy genetic algorithm (NGA), for cost-effective sampling network design in the presence of uncertainties in the hydraulic conductivity (K) field. Both methodologies couple a genetic algorithm (GA) with a numerical flow and transport simulator and a global plume estimator to identify the optimal sampling network for contaminant plume monitoring. The MCSGA approach yields one optimal design each for a large number of realizations generated to represent the uncertain K-field. A composite design is developed on the basis of those potential monitoring wells that are most frequently selected by the individual designs for different K-field realizations. The NGA approach relies on a much smaller sample of K-field realizations and incorporates the average of objective functions associated with all K-field realizations directly into the GA operators, leading to a single optimal design. The efficacy of the MCSGA-based composite design and the NGA-based optimal design is assessed by applying them to 1000 realizations of the K-field and evaluating the relative errors of global mass and higher moments between the plume interpolated from a sampling network and that output by the transport model without any interpolation. For the synthetic application examined in this study, the optimal sampling network obtained using NGA achieves a potential cost savings of 45% while keeping the global mass and higher moment estimation errors comparable to those errors obtained using MCSGA. The results of this study indicate that NGA can be used as a useful surrogate of MCSGA for cost-effective sampling network design under uncertainty. Compared with MCSGA, NGA reduces the optimization runtime by a factor of 6.5.

Keywords: Contaminant transport; Monitoring network design; Spatial moment analysis; Noisy genetic algorithm; Monte Carlo analysis; Uncertainty

1. Introduction

Since the early 1980s, the coupled simulation-optimization model has increasingly become a valuable tool for analyzing groundwater systems and managing groundwater resources [1,8,13,19,27,34,41,48–50,56]. A primary motivation for the development of simulation-optimization models is the high costs associated with groundwater quality management. A representative simulation-optimization model is one that seeks to identify the least-cost strategy to meet specified constraints. In recent years, the least-cost strategies are usually associated with pump-and-treat or bioremediation design [2,5,30, 46,55].

* Corresponding author. Tel.: +1 205 348 0579; fax: +1 205 348 0818.
E-mail address: czheng@ua.edu (C. Zheng).

0309-1708/$ - see front matter © 2005 Elsevier Ltd. All rights reserved.
doi:10.1016/j.advwatres.2005.08.005

Groundwater remediation often has time horizons of 30 years or longer. Thus long-term monitoring of a remediation system's performance is essential to ensure that the remediation objectives are being achieved and the risks to human health and environment are being properly managed [9]. Over-sampling is a common problem encountered in groundwater quality monitoring, where data collection and analysis of long-term monitoring are expensive. Although the cost for an individual sampling data point may be relatively small, the scale of the required data collection effort over time can make the cumulative costs very high. For a typical groundwater contamination site, several hundred samples may be collected and analyzed each year that may cost hundreds of thousands of dollars. To prevent over-sampling, applications of simulation-optimization models to long-term sampling network design can lead to substantial cost savings by eliminating or minimizing unnecessary samples [9]. This paper is intended to address simulation-optimization modeling for cost-effective groundwater sampling network design in the presence of uncertainties in the hydraulic conductivity field.

Groundwater sampling network design has been studied extensively in the past [3,4,6,10,11,21–23,25,29,31,32,36,39,42,43,51], and more recently the efforts have often focused on the least-cost strategies [43,39,51]. The optimization of sampling network design can be accomplished using a variety of approaches as summarized in [35]. Selecting an appropriate method involves numerous criteria, the most important of which include site-specific long-term performance objectives and the amount and type of available data. Reed et al. [39] presented an optimization methodology in which a genetic algorithm is coupled with a flow and transport simulator and a global mass estimator to search for optimal sampling strategies. Wu et al. [54] extended the methodology of Reed et al. [39] by introducing the first and second moments of a plume as additional constraints into the optimization formulation. The methodology developed by Reed et al. [39] and extended by Wu et al. [54] does not address uncertainties in the hydraulic conductivity field.

In reality, there always exists some amount of uncertainty in an aquifer simulation model. One of the most important parameters, in terms of its contributions to uncertainty, is hydraulic conductivity (K). In particular, the transport of contaminants in groundwater is dominated by the spatial variation of hydraulic conductivity. Sampling decisions will have to be made under consideration of uncertainties in the aquifer simulation model, and the reliability of model-based sampling decisions will be a function of model uncertainties. A commonly used approach to dealing with the uncertainty in the K-field is the conditional Monte Carlo simulation based on a certain number of measured hydraulic conductivity data [12,26,31,32,47]. Although a number of studies have incorporated uncertainties into the simulation-optimization model to design cost-effective sampling networks and determine the reliability of plume detection in clean-up systems of landfills and hazardous waste sites [11,31,32,47], the fundamental objectives of those studies are substantially different from the goal of this study.

This study is intended to evaluate and compare two methodologies for cost-effective sampling network design under consideration of uncertainty. Both methodologies couple a genetic algorithm with a numerical flow and transport simulator and a global plume estimator to identify the optimal sampling network for contaminant plume monitoring. Because a simple genetic algorithm cannot address uncertainty directly, other techniques such as Monte Carlo simulation, stacking of K-field realizations, and chance constraints [5,15,32,37] must be used to incorporate uncertainty into a simple genetic algorithm. For the first methodology used in this study, the Monte Carlo approach is adopted to generate a large number of equally likely realizations of the K field to account for the effect of uncertainty on optimal network design. For the second methodology, a noisy genetic algorithm is adopted which was developed specifically to deal with uncertainty.

Unlike Monte Carlo simulation that requires a large number of samples to be drawn from the probability distribution of the K-field to achieve sufficient accuracy, a noisy genetic algorithm can work well without extensive sampling from the realizations of the K-field [18,33,44,46]. Smalley et al. [46] successfully coupled a noisy genetic algorithm with a flow and transport model for predicting concentrations in a risk-based in situ bioremediation design system. Gopalakrishnan et al. [18] used a noisy genetic algorithm to identify the optimal groundwater remediation design based on the assessment of risks to human health. To date, noisy genetic algorithms have only been applied to remediation design associated with groundwater quality management [18,46]. This study thus represents a first attempt to apply a noisy genetic algorithm to sampling network design under uncertainty. To gain confidence in the applicability and usefulness of noisy genetic algorithms in solving sampling network design problems, this paper presents a detailed comparison between a noisy genetic algorithm and the Monte Carlo based approach.

This paper is organized in five sections. Following this introduction, we provide a brief overview of the simulation-optimization model used in this study for sampling network design under deterministic conditions. We then discuss two methodologies, Monte Carlo simple genetic algorithm and noisy genetic algorithm, for incorporating uncertainties into the deterministic simulation-optimization model. Next we illustrate the two methodologies and compare their performance in an application to a synthetic aquifer system. Finally we summarize the findings and offer some concluding remarks.

2. Optimal monitoring network design

Wu et al. [54] presented a simulation-optimization methodology for cost-effective sampling network design under deterministic conditions. Their methodology is an extension of Reed et al. [39] and is based on the minimization of total monitoring (capital and sampling) costs subject to two accuracy constraints. For the sake of completeness, the methodology of Wu et al. [54] is briefly recapitulated in this section. For more detailed information, refer to Wu et al. [54] and Reed et al. [39].

2.1. Numerical simulation and global plume estimation

The first step in the methodology of Wu et al. [54] is the development of flow and transport models for the study site. This study utilizes the flow and transport models based on the three-dimensional finite-difference flow code, MODFLOW [20,28], and its solute transport companion, MT3DMS [57]. The flow and transport codes are used to simulate the contaminant plume from the initial time to the end of the anticipated monitoring period. The simulated plume represents the future conditions to be monitored. If a model node is selected as a potential monitoring well location, the simulated concentration value at that location is considered known.

The second step is to use the known concentrations at all potential monitoring well locations to construct an approximate new plume through interpolation. The interpolated plume is then compared, in terms of both total mass as well as first and second moments, with the simulated plume output from the transport model without any interpolation. If enough nodes are selected as potential monitoring well locations, the difference between the simulated and interpolated plumes would be minimal. On the other hand, the more model nodes are selected as potential monitoring well locations, the higher the capital and sampling costs would be. Thus there exists a tradeoff between the accuracy of the interpolated plume based on the sampled data and the cost-effectiveness of the sampling network.

An interpolation method, ordinary kriging (OK) [14], is applied to estimate contaminant concentrations at all unsampled nodes within the model domain. Then the OK-interpolated concentrations can be used for global plume estimation to compare with that determined from the concentration distributions directly output from the transport model without any interpolation. In this study, the global plume estimation relates to three moments, including the zeroth, first and second moments. The zeroth moment represents the global mass of the plume. The first and second moments specify the centroid of the plume and the spread of the plume around its centroid, respectively [16,36].

2.2. Objective function and constraints

The third step in the methodology of Wu et al. [54] is the formulation of an optimization model. The objective of the optimization model is to minimize the total monitoring (installation/drilling and sampling) costs while maintaining the accuracy of global plume estimation based on the sampled data. The monitoring network design problem can thus be formulated as an optimal control model with an objective function and a set of constraints [54]:

$$\min \quad J = \alpha_1 \sum_{i=1}^{n} x_i l_i + \alpha_2 \sum_{i=1}^{n} y_i d_i \tag{1}$$

$$\text{subject to} \quad e_{mass} \leqslant \varepsilon_1 \tag{2}$$

$$e_{1\text{st}} \leqslant \varepsilon_2 \tag{3}$$

$$e_{2\text{nd}} \leqslant \varepsilon_3 \tag{4}$$

where, in the objective function as given in (1), J is the management objective representing the total costs for sampling and well installation/drilling, n is the total number of potential monitoring wells; α_1 is the cost for each sampling, x_i is a binary variable indicating whether sampling takes place at well i (yes if $x_i = 1$; no if $x_i = 0$), l_i is the number of sampling at different elevations for well i. If sampling takes place at well i, the well i is selected to be sampled at multiple (i.e., l_i) elevations. α_2 is the fixed capital cost for installation/drilling per unit depth of well i, d_i denotes the depth of borehole associated with well i, and y_i is a binary variable indicating whether well i is drilled (yes if $y_i = 1$; no if $y_i = 0$).

The first constraint as expressed in Eq. (2) requires that the discrepancy, e_{mass}, be smaller than a prescribed error tolerance, ε_1, between the global mass of the complete solute plume as predicted by the solute transport model and that of the approximate solute plume interpolated from the sampled data at the installed monitoring wells. The second and third constraints in Eqs. (3) and (4) require that both 1st and 2nd spatial moments of the complete and approximate solute plumes as described above agree with each other within two sets of pre-determined criteria, ε_2 and ε_3, respectively. $e_{1\text{st}}$ and $e_{2\text{nd}}$ are the weighted sum of errors for the respective first and second moment estimations. Mathematically, the three constraints can be written as

$$e_{mass} = \left| \frac{M_0 - M_j}{M_0} \right| \tag{5}$$

$$e_{1\text{st}} = \sum_{k=1}^{nd} \left| \frac{u_{0,1}^k - u_{j,1}^k}{u_{0,1}^k} \right| \omega_1^k \tag{6}$$

$$e_{2\text{nd}} = \sum_{k} \left| \frac{u_{0,2}^k - u_{j,2}^k}{u_{0,2}^k} \right| \omega_2^k \tag{7}$$

where M_0 is the contaminant mass in the area of interest as determined by the transport model, and M_j is the

approximate mass in the same area as determined by the global mass estimator based on the sampling design j, $u_{0,i}$ is the first or second moment of the simulated plume as output from the transport model, $u_{j,i}$ is the corresponding moment estimated on the basis of the sampling design j, i denotes the order of moment (i.e., first or second moment), nd denotes the dimension of the plume and is equal to 2 or 3, depending on the type of the flow and transport model, k is the direction along which the moment is computed, and ω_i^k is the weight assigned to the ith moment in the k-direction. For a three-dimensional problem, the second moment includes nine component terms (reduced to six due to symmetry), whereas in a two-dimensional system, the second moment has only three component terms.

The constrained optimization problem as defined in Eqs. (1)–(4) can be transformed into an easier-to-solve unconstrained one by adding the amount of any constraint violation to the fitness function as a penalty. This is accomplished in this study by modifying Eqs. (1)–(4) as

$$\min F = J + P_1 + P_2 \tag{8}$$

with

$$P_1 = \beta_1 \frac{e_{mass} - \varepsilon_1}{\varepsilon_1} + \beta_2 N_{\text{unestimate}}, \quad \varepsilon_1 > 0 \tag{9}$$

$$P_2 = \beta_3[(e_{1\text{st}} - \varepsilon_2) + (e_{2\text{nd}} - \varepsilon_3)] \tag{10}$$

where F is the penalized fitness value; P_1 and P_2 are the penalty amounts of constraint violation with respect to the global mass and higher moment estimation errors, respectively; $N_{\text{unestimate}}$ is the number of points at which the concentration is not estimated as a result of no sampling data point within the specified search radius, and β_i $(i = 1, 2, 3)$ is penalty coefficients. The specified search radius is defined a maximal distance of search for known data (concentrations) around an unestimated point.

2.3. Solution by genetic algorithms

The final step in the methodology of Wu et al. [54] is to find the optimal sampling plan from among many alternatives using the genetic algorithm (GA) [17,38, 45]. In recent years, GA has been shown to be a valuable tool for solving complex optimization problems in broad fields, including groundwater management and monitoring network design [2,7,11, 24,30,40,51–53,55]. For any sampling network design problem, a number of potential sampling locations may be specified. The GA considers each sampling alternative design to be a string (chromosome) consisting of zero-one variables, where the value of 1 in the ith digit (bit) represents sampling from the ith potential location, and 0 no sampling. The total number of nonzero digits in the string denotes the number of sampling locations used in the current design. In this study, a simple GA procedure was used that consisted of 60 generations with a population of 800 individuals (chromosomes) in each generation. For a more thorough discussion of using GA in the context of sampling network design, refer to [39,54].

3. Methodologies for dealing with uncertainty

A simple genetic algorithm (SGA) cannot explicitly address the uncertainty in the aquifer simulation model arising from insufficient hydraulic conductivity data. Methodologies for dealing with uncertainty in optimization modeling are reviewed by Freeze and Gorelick [15]. This study evaluates and contrasts two methodologies in the context of monitoring network design. First, SGA is combined with Monte Carlo simulation in what is referred to as Monte Carlo simple genetic algorithm (MCSGA). Second, SGA is applied in a noisy environment in what is referred to as noisy genetic algorithm (NGA) [18,33,46].

3.1. Monte Carlo simple genetic algorithm

A commonly used stochastic approach for accommodating the uncertainty arising from insufficient hydraulic conductivity data needed for a groundwater model is Monte Carlo simulation in which multiple realizations of the hydraulic conductivity field are generated [12,31,32,47]. Each realization is equally likely in the statistical sense, and can be further conditioned to the same set of known hydraulic conductivity data. The flow and transport model must be run for each K realization, leading to a range of calculated head and concentration distributions. It is noteworthy that several assumptions are associated with the Monte Carlo methodology applied in this study, including, (1) the hydraulic conductivity field follows a log-normal distribution, (2) the hydraulic conductivity field is ergodic and has stationary second moment, and (3) the spatial correlation is defined as an isotropic, exponential covariance function [46].

For each realization of the hydraulic conductivity field, the sampling network design problem becomes a deterministic one and can be solved independently using the simple genetic algorithm as described in Section 2. In this manner, the optimal or near-optimal designs corresponding to all realizations of the K-field can be obtained and evaluated. These designs are interim, each of which only satisfies the constraints associated with a particular K realization. Subsequently, a composite design can be developed on the basis of those potential monitoring wells that are most frequently selected by the individual interim designs for different K realizations. Since several hundred or more K realizations may be required for adequate representation of the uncertainty in the K-field, the MCSGA approach is time

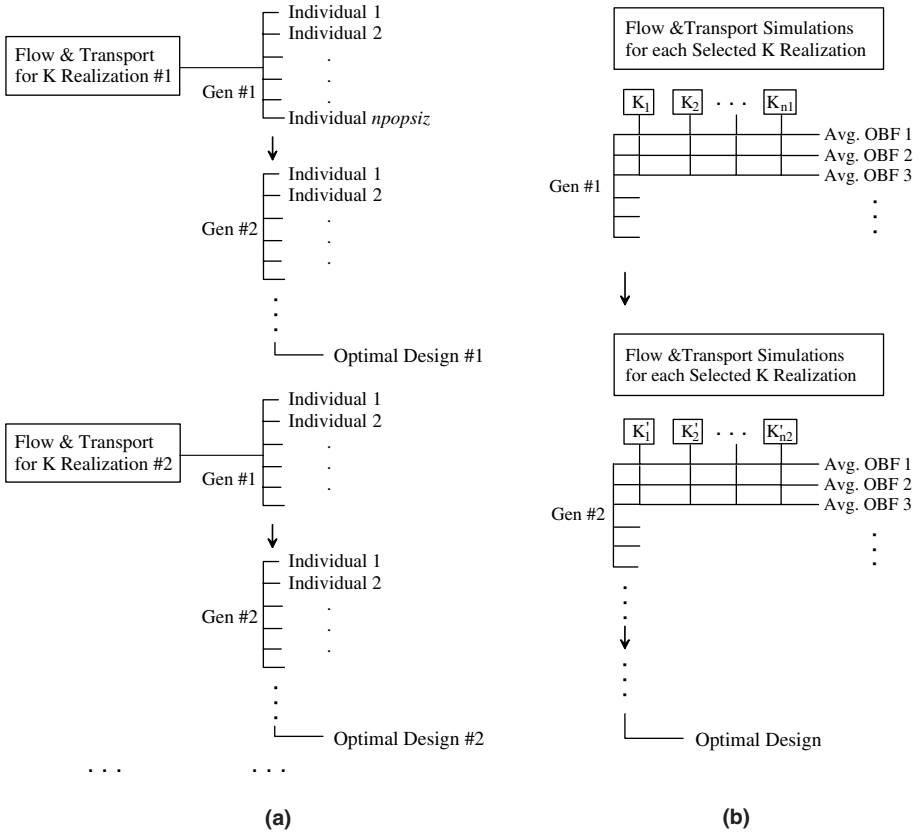

Fig. 1. Schematics of the two methodologies used in this study for dealing with uncertain hydraulic conductivity in monitoring network design optimization: (a) Monte Carlo simple genetic algorithm (MCSGA), and (b) noisy genetic algorithm (NGA). Note that *npopsiz* is the size of GA population, and 'Gen' is the abbreviation for GA generation. K_1 in the rectangular box refers to running the flow and transport model for the conditional realization K_1. 'Avg. OBF1' is the average objective function value for individual No. 1.

consuming. A simplified flow chart of the MCSGA approach is given in Fig. 1(a).

3.2. Noisy genetic algorithm

The noisy genetic algorithm (NGA) is a relatively new search technique that allows a simple genetic algorithm to operate in a noisy environment [18,33,44,46]. In the context of this study, a noisy environment means that the fitness measure of a given trial monitoring design (chromosome) cannot be evaluated accurately because of the effect of K variability on the plume transport. As a result, a special type of fitness function, referred to as sampling fitness function, is utilized that is based on the averaging of fitness function values for multiple realizations of the K-field. Unlike Monte Carlo simulation that requires extensive realizations drawn from probability distributions to obtain reasonably accurate results, NGA has been shown in afore-mentioned studies to perform well without sampling a large number of K realizations. According to the Central Limit Theorem, the fitness function for a given trial monitoring design will reduce the amount of noise by taking the mean of multi-sampling fitness evaluations [18,46].

The main difference between NGA and a simple GA is that the fitness function for a single generation in the former is the average of function evaluations obtained from multiple hydraulic conductivity realizations. The population in each generation contains many individuals representing different interim network designs. The noisy fitness for each individual is found by evaluating it for several realizations, and is compared with those of others within the population. As the generation evolves, those individuals with the highest noisy fitness function values will dominate the population. Because only those individuals with high fitness under all selected hydraulic conductivity realizations are able to dominate, the procedure will converge to optimal solutions with high fitness even when only a few sample realizations of the K-field are drawn for each design.

In Eqs. (5) and (6), M_0 is the contaminant mass in the model domain determined by the transport model; and $u_{0,1}$ and $u_{0,2}$ are the first and second moments of the calculated plume as output from the transport model, respectively. For each realization of the K-field, different values of both $u_{0,1}$ and $u_{0,2}$ are determined, which presents a difficulty when NGA is applied to the monitoring network design problem. This is because reasonably

accurate and stationary values of $u_{0,1}$ and $u_{0,2}$ are needed as common references for comparison of potential designs associated with different hydraulic conductivity realizations. To overcome this difficulty, it is assumed that $u_{0,1}$ and $u_{0,2}$, along with M_0, can be determined from the plume resulting from the kriged K-field based on the measured K data at a set of known locations. This assumption is consistent with the practice in which the K distribution for a field-scale model is often interpolated from the measured data by the kriging method and used as the basis for monitoring network design. Fig. 1(b) illustrates the framework used in this study for cost-effective monitoring network design based on NGA.

In this study, K-field sampling is done through a random number generator with each random number corresponding to a particular realization among all the realizations generated a priori. A potential monitoring design is evaluated for each K realization by running the flow and transport model and determining the objective function and constraint violations. Then the overall fitness of any given potential design is set to the average of its fitness values associated with every selected K realization [18,46].

Note that the methodologies presented in this study identify the optimal sampling design for only one monitoring period. For the monitoring network design problems with multiple monitoring periods, the value of y_i in Eq. (1) is 1 when the ith monitoring location is selected for a particular monitoring period; and the value of y_i remains 0 for all other periods since the capital cost should be counted only once. Also, the fixed capital cost is generally more expensive than the sampling cost at any monitoring location, and thus the network design for one monitoring period affects those of other periods. Accordingly, for the multi-period monitoring network design problems, the optimal network designs for different monitoring periods are not independent.

4. Application to a synthetic aquifer system

4.1. Description of the application

The hypothetical application used in this study involves a two-dimensional confined aquifer measuring 600 m long in the x-direction and 400 m wide in the y-direction. Fig. 2 shows the plan view of the synthetic aquifer and the block-centered finite difference mesh. The aquifer is surrounded by a constant-head boundary along the left side, a specified-flux boundary with a constant inflow rate along the right side, and no-flow boundaries along the upper and lower sides. The hydraulic conductivity distribution in the aquifer is isotropic and represented by a log-normally distributed, spatially-correlated random field. Other properties in-

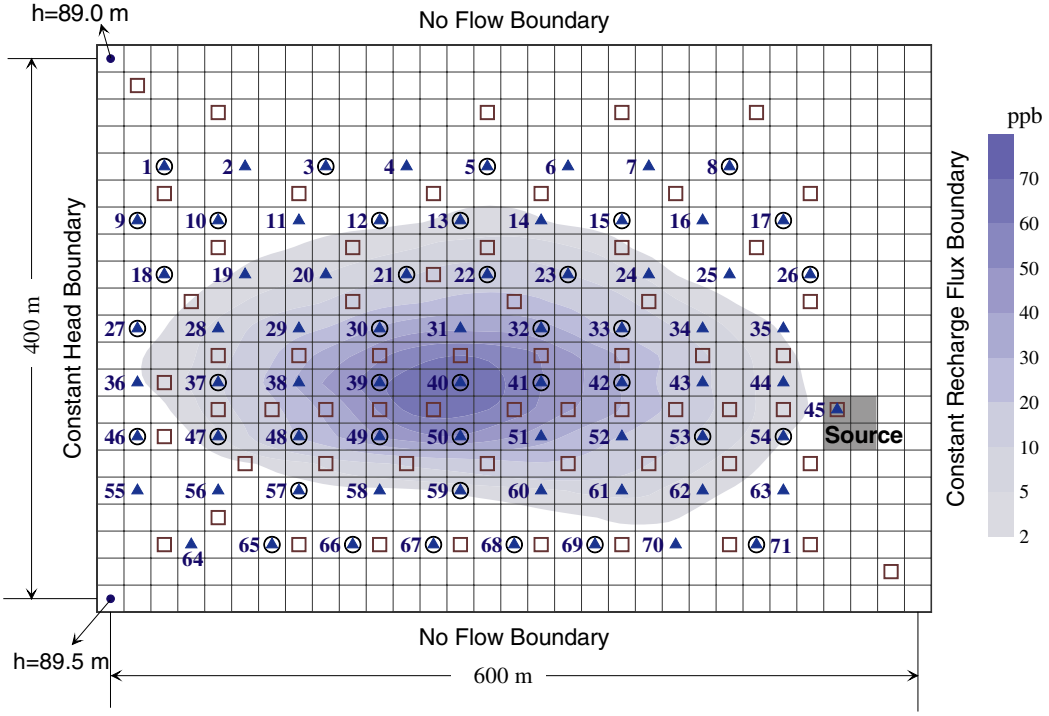

Fig. 2. Configuration of the monitoring network design problem. The solid triangles indicate the pre-defined potential monitoring well locations. The open circles denote the optimal monitoring wells selected by NGA. The color-filled contour map represents the concentration distribution at the end of the monitoring period output by the transport model for the hydraulic conductivity field kriged using 62 known K values (shown as open squares).

Table 1
Primary input data used in this study[a]

Parameter	Value
Porosity	0.175
Aquifer thickness	10.0 m
Longitudinal dispersivity	8.5 m
Ratio of horizontal transverse to longitudinal dispersivity	0.1
Constant flux along the specified-flow boundary	9.45 m/day
Mean of $\ln K$	2.2 m/day
Variance of $\ln K$	0.30
Correlation scale of hydraulic conductivity	100.0 m
Grid spacing along column	20.0 m
Grid spacing along row	20.0 m

[a] Modified from Wagner [51].

cluding porosity, thickness, and dispersivities are constant throughout the aquifer system. Key input data used in the flow and transport model and K field generation are listed in Table 1. The flow and transport model for the application is based on a version of MODFLOW [28] and MT3DMS [57] codes.

Sequential Gaussian simulation (SGSIM) [14] was used to generate 1000 equally likely realizations of the K-field, based on the $\ln K$ statistical parameters (mean, variance, and correlation length) listed in Table 1. The hydraulic conductivity was assumed to be known at 62 measurement locations (see scattered square symbols in Fig. 2) within the aquifer, with the mean and variance of $\ln K$ equal to 2.2 and 0.3, respectively. The K values ranged from a minimum of 2.6 m/day to a maximum of 30.0 m/day. All 1000 K realizations were conditioned to the 62 K data.

An instant spill was assumed to occur at the source area ($c_0 = 1000.0$ ppb) that resulted in a contaminant plume migrating toward the left boundary (see Fig. 2). The plume shown in Fig. 2 was obtained by the transport model for the K-field kriged from the 62 known K data. The total simulation time was three years, the monitoring period considered in this application. A total of 71 potential monitoring locations were initially selected as shown in Fig. 2. The total mass and the first and second moments for the interpolated plume based on the 71 monitoring locations were in reasonably close agreement with those calculated directly from the output of the transport model.

In this study, the operational cost for sampling ($\alpha_1 l_i$) and the fixed cost for installation/drilling ($\alpha_2 d_i$) were both taken to be \$2000 for each monitoring well. Wu et al. [54] pointed out that the penalty costs set approximately 5–20 times the expected real monitoring costs would result in an optimal or near-optimal sampling design that is both cost-effective and sufficiently accurate in terms of mass and higher moment estimations. Moreover, the number of sampling data is always much smaller than the total number of model nodes in a numerical simulation model, thus it is rather difficult to reduce the second moment estimation errors, making it necessary to set the error tolerance for the plume moment constraints as small as possible [54]. Considering this approximate rule of setting penalty coefficients and the expected number of monitoring wells in this example, the coefficients for the fitness objective function given in Eqs. (8)–(10) were set as follows: $\beta_1 = 5.0 \times 10^4$, $\beta_2 = 50$, $\beta_3 = 3.0 \times 10^5$, $\varepsilon_1 = 0.05$, and $\varepsilon_2 = \varepsilon_3 = 0$. All weights assigned to the higher moments along different directions are set equal, i.e., $\omega_i^k = 1$ in Eqs. (6) and (7).

4.2. Solution based on Monte Carlo simple genetic algorithm

For each conditional realization of the K-field, the simple genetic algorithm was applied to identify a monitoring network that is optimal specific to the associated K realization. As a result, a total of 1000 individual optimal designs were obtained corresponding to 1000 K realizations. Fig. 3 shows how frequently each of the 71 potential monitoring wells is selected by any of the 1000 individual optimal designs. From a comparison of Figs. 3 and 2, it is evident that the monitoring wells either close to the plume centroid or near the edges have a greater probability of being chosen by one or more optimal designs. This is because overall the interpolated plume based on those monitoring wells is more likely to match the plume directly output from the transport model.

Fig. 4 is a scatter diagram showing the relative errors of the interpolated plume based on each monitoring network for a corresponding K realization. The relative errors are expressed in terms of the differences in global mass and higher moments between the interpolated plume and the reference plume output by the transport model without any interpolation. The average relative errors of global mass and first moments for all monitoring designs are quite small, at 4.17% and

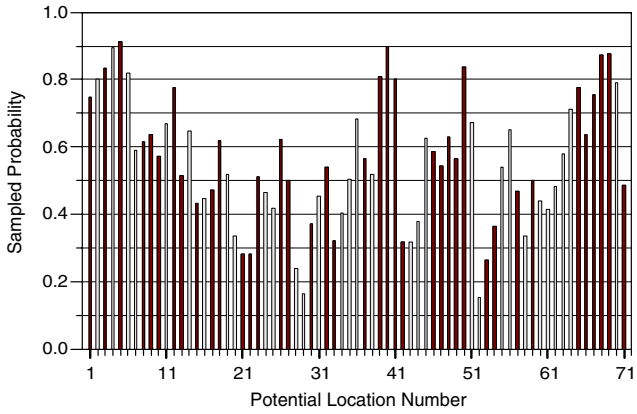

Fig. 3. Relative frequency of each pre-defined potential monitoring well selected by the individual optimal designs obtained using MCSGA for 1000 conditional realizations of the K-field. The columns of shaded color denote the optimal monitoring locations selected by NGA.

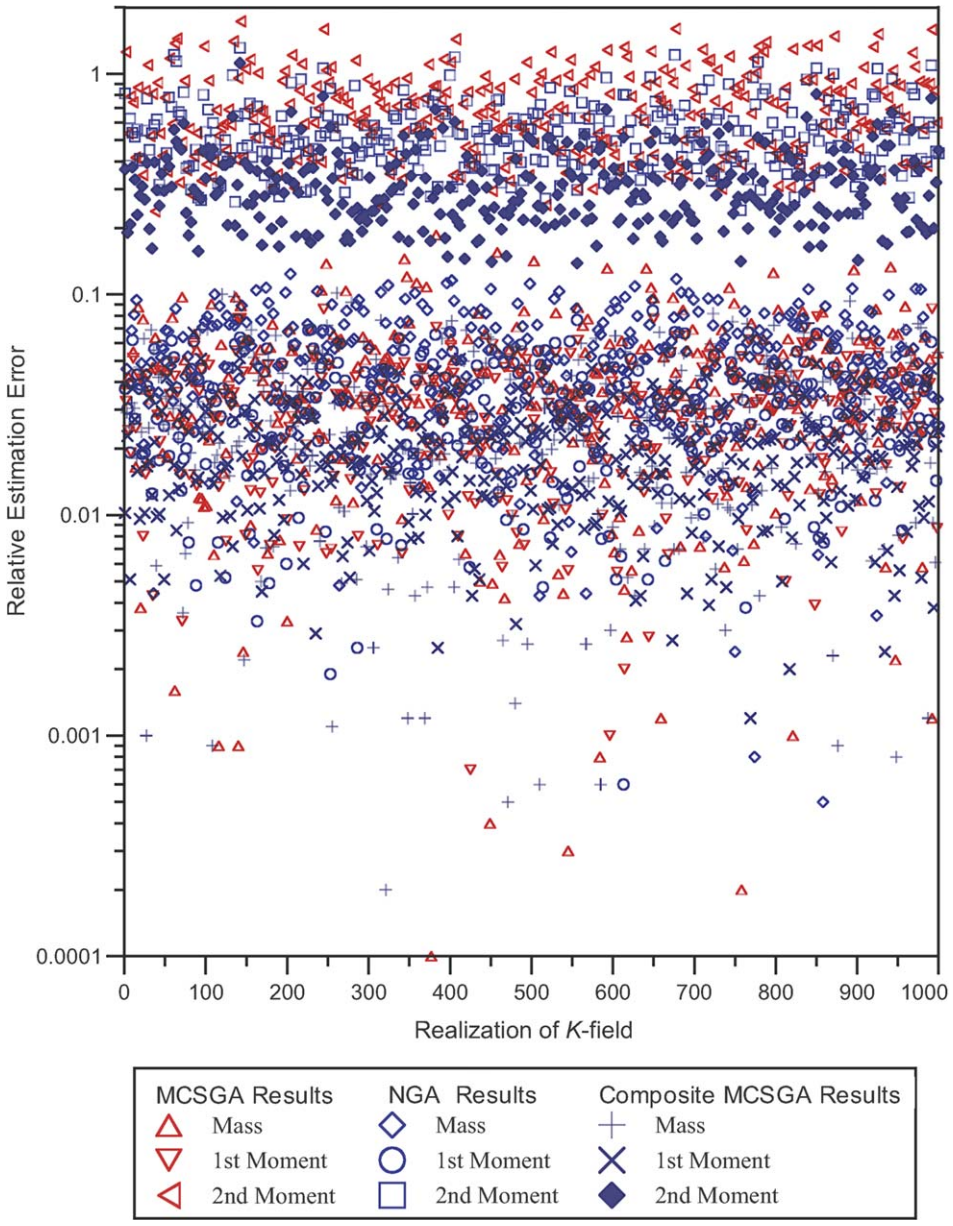

Fig. 4. Comparison of relative estimation errors of global mass and higher moments for 1000 realizations of the *K*-field under different network design methodologies. The errors are computed as the relative differences between the plume interpolated from the optimal monitoring wells and that given by the transport model without any interpolation for 1000 conditional realizations of the *K*-field.

Table 2
Statistics of relative estimation errors for optimal monitoring network designs obtained using different methodologies

Item[a]	MCSGA			Composite MCSGA			NGA		
	mass	μ_1	μ_2	*mass*	μ_1	μ_2	*mass*	μ_1	μ_2
Minimum	0.0000	0.0007	0.2348	0.0000	0.0006	0.1247	0.0000	0.0006	0.2321
Maximum	0.3180	0.0860	1.8290	0.1287	0.0671	1.1909	0.1566	0.0844	1.4825
Mean	0.0417	0.0293	0.6965	0.0312	0.0189	0.3151	.0547	0.0309	0.5397
Standard deviation	0.0323	0.0150	0.2901	0.0230	0.0103	0.1239	0.0277	0.0156	0.1913

[a] The items of *mass*, μ_1 and μ_2 represent the relative estimation errors for the mass, first and second moments of the plume, respectively.

2.93%, respectively, but that of second moments is substantially larger at 69.65% (Table 2). This can be attributed to the significant variation of plume shape caused by the variability in the *K*-field.

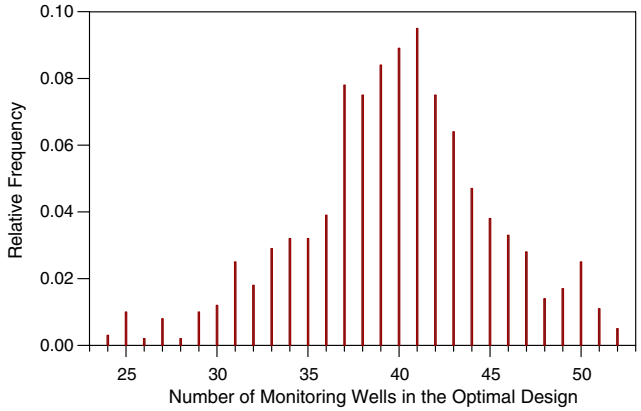

Fig. 5. Distribution of the number of monitoring wells selected by each optimal monitoring network design obtained using MCSGA for 1000 conditional realizations of the *K*-field.

Fig. 5 shows the distribution of the number of monitoring wells in each optimal design for a corresponding realization of the *K*-field. There are, on average, 40 monitoring wells, which represent a 43.66% potential cost savings compared with the costs for the initially selected 71 potential wells. The standard deviation of the distribution is 5 wells, with a minimum of 24 and a maximum of 52. Correspondingly, the former represents a maximum potential cost savings of 66.20% and the latter a minimum cost savings of 26.76%.

Based on the individual optimal designs obtained for different *K* realizations, a single composite design may be developed which would be optimal, in an average sense, given the uncertainty represented by the 1000 *K* realizations. Since there is an average of 40 monitoring wells in all individual designs as shown in Fig. 5, the 40 monitoring wells with the highest probabilities of selection by any individual design (from a maximum of 0.914 to a minimum of 0.518) were designated as the composite optimal design. The composite design of 40 wells was then applied to all 1000 *K* realizations. The resulting average relative errors of global mass and higher moments are also shown in Fig. 4 and Table 2. From a comparison of scattered errors in Fig. 4, it can be seen that the error distributions are similar between the individual optimal designs for corresponding *K* realizations and the single composite design applied to the same *K* realizations. The most notable difference between the two is that the average relative error of second moments decreases significantly for the composite design. These results confirm the validity of the composite design as a superior representative of the individual designs optimized independently for each of the 1000 *K* realizations.

4.3. Solution based on noisy genetic algorithm

Smalley et al. [46] concluded that an effective strategy for *K*-field sampling in NGA is to use smaller sample sizes for early generations followed by larger sample sizes in later generations. This strategy was adopted in this study. The number of *K*-field realizations was set to five realizations for the first four generations and increased by five realizations every four generations afterward until the maximum of 30 realizations was reached. From trial runs, it was determined that 30 *K*-field realizations and 40 generations were sufficient to identify an optimal or near-optimal monitoring network design.

The monitoring wells selected by the optimal network design obtained using NGA are shown in Fig. 3 as color-filled columns; their locations relative to the plume are shown in Fig. 2. It is noteworthy that most of the wells selected by NGA also have a greater probability of being selected by MCSGA. The optimal monitoring network identified by NGA includes 39 monitoring wells, which corresponds to a potential cost savings of 45.07% compared with the costs for the initially selected 71 potential wells. Furthermore, the NGA-based optimal design of 39 wells has one fewer well than the MCSGA-based composite design of 40 wells.

To investigate the robustness of the NGA-based optimal design, it was applied to the 1000 *K* realizations generated previously for Monte Carlo simulation to compute the relative errors of global mass and higher moments under each of the 1000 *K* realizations. The relative errors are expressed in terms of the differences between the interpolated plume based on the monitoring network and the reference plume output by the transport model under the kriged *K*-field. For the sake of comparison, the scattered distribution of relative errors, with an average of 5.47% for global mass and 3.09% and 53.97% for first and second moments, respectively, is also shown in Fig. 4. The comprehensive key statistics of relative errors for all the network designs obtained using different methodologies is listed in Table 2.

4.4. Comparison and discussion

From the first glance of Fig. 4, it is difficult to differentiate the relative errors of global mass and first moment for the NGA-based optimal design applied to 1000 different *K* realizations from those for both MCSGA-based individual optimal designs and the composite 40-well design. The error distribution in terms of global mass and first moment for the NGA-based optimal design is very similar to those for both the MCSGA-based individual designs and the composite design. However, the distribution of the relative error in terms of second moment for the three different sets of designs is clearly distinct from one another. On the whole, the relative errors of second moments for the NGA-based optimal design are relatively larger than those of the MCSGA-based composite design for different *K* realizations and smaller than those of the individual optimal designs obtained using MCSGA for different

K realizations. As shown in Table 2, the average relative errors of global mass, first and second moments are 4.17%, 2.93% and 69.65%, respectively, for the individual optimal designs obtained using MCSGA for the 1000 K realizations. The average relative errors of global mass and first moments are sufficiently small. However, due to significant variations in K realizations to which the second moments are very sensitive, the average relative error of second moments is substantially larger. The MCSGA-based 40-well composite design has average relative errors of 3.12%, 1.89%, and 31.51% for global mass, first and second moments, respectively, which are lower than those computed for the individual optimal designs. Thus the composite design can be considered an optimal representative of the 1000 individual optimal designs. The single optimal design obtained using NGA, when applied to the same 1000 K realizations, resulted in average relative errors of 5.47%, 3.09%, and 53.97% for global mass, first and second moments, respectively. The average relative errors of global mass and first moment for the NGA optimal design are close to those for both MCSGA-based individual optimal designs and the composite 40-well design. However, the average relative error of second moments for the NGA optimal design is smaller than that of the MCSGA-based individual optimal designs, but larger than that of the MCSGA-based composite 40-well design.

To further validate the result from the NGA, Fig. 6 shows a visual comparison of the histograms (discrete probability density function or discrete PDF) and cumulative distribution function (CDF) for relative errors of global mass, first and second moment estimates, respectively. Fig. 6(a) indicates that the range of distribution for the global mass errors based on the NGA design is close to that based on the MCSGA individual designs, even though the former has an greater mean than the latter (5.47% vs. 4.17%). Overall, the differences among MCSGA-based and NGA-based designs are insignificant. Fig. 6(b) shows the distribution of the first moment errors. The difference between the NGA- and MCSGA-based designs is almost negligible. While the error distribution for the MCSGA-based composite 40-well design is defined more narrowly and sharply, the overall distributions for the first moment errors are similar and sufficiently small for all three cases. Fig. 6(c) shows the differences among the three cases for the second moment errors. The MCSGA-based composite 40-well design is most satisfactory, with smaller errors than both the NGA-based design and MCSGA-based individual designs. However, the shape of CDF for the NGA-based design is similar to that for the MCSGA-based composite 40-well design, which is sharper than that for the MCSGA-based individual designs. Also, compared with the MCSGA-based individual designs, the error distribution for the NGA-based design has a smaller mean and narrower range. Overall, the optimal design identified by NGA appears to be an acceptable surrogate for the MCSGA-based designs.

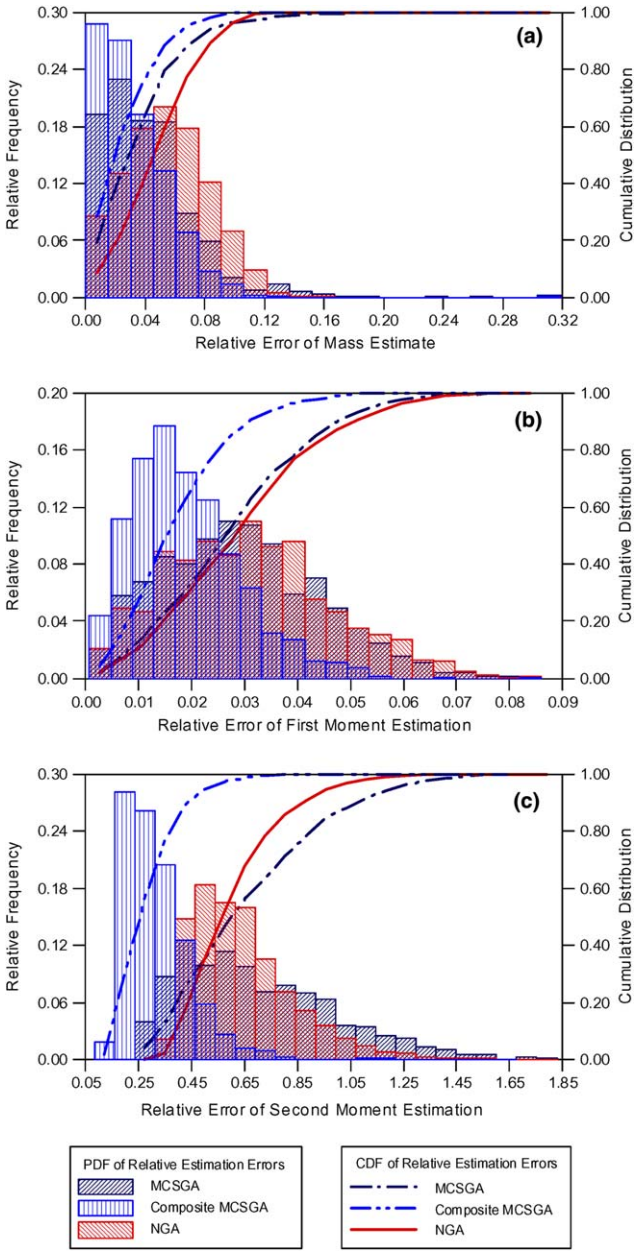

Fig. 6. Comparison of relative estimation errors of global mass and higher moments in terms of PDF and CDF for optimal network designs obtained using different methodologies.

Computationally, NGA is much more efficient than MCSGA. In this study, completion of an optimization run based on MCSGA requires a total run time of approximately 170 hours on a desktop PC equipped with a 2.20 GHz Pentium-4 CPU. In contrast, the completion of a run based on NGA requires only 26 hours on the same PC. For real-world applications, MCSGA may become computationally prohibitive. The results of this study show that NGA can find the near-optimal

sampling design, and the distribution of global mass and higher moment estimation errors based on the NGA design have statistical traits similar to those based on MCSGA. Thus with its computational efficiency and robustness, NGA may represent a promising alternative to MCSGA for real-world applications to design the most cost-effective groundwater monitoring networks under uncertainty.

5. Conclusions

We have evaluated and compared two methodologies, Monte Carlo simple genetic algorithm (MCSGA) and noisy genetic algorithm (NGA), for incorporating the uncertainty in the *K*-field into cost-effective monitoring network design problems. Both methodologies couple a genetic algorithm with a numerical flow and transport simulator and a global plume estimator to identify the optimal sampling network for contaminant plume monitoring. However, they differ in the handling of the *K*-field uncertainty. MCSGA utilizes a sufficiently large number of realizations of the *K*-field for adequate uncertainty representation, and identifies an optimal monitoring network design for each realization. A limitation of this approach is that the multiple designs cannot be applied directly to a real field application. A composite design, however, can be developed on the basis of those potential monitoring wells that are most frequently selected by individual designs under different *K*-field realizations. NGA, on the other hand, relies on a much smaller sample of *K*-field realizations, and incorporates the average of objective functions associated with all *K*-field realizations into the GA operators, to identify a single optimal design.

For the application example examined in this paper, the optimal network design obtained using NGA achieves a potential cost savings of 45.07% while maintaining acceptable accuracy in global mass and higher moment estimations. The estimation error distributions obtained by applying the NGA optimal design to multiple realizations of the *K*-field closely agree with those obtained by applying the simple genetic algorithm to all individual realizations of the *K*-field (MCSGA). This indicates that NGA can be used as an effective surrogate of MCSGA for cost-effective monitoring network design under uncertainty. Compared with MCSGA, NGA is much more efficient computationally, by a factor of 6.5 for this study, and results in a unique solution.

While this study has demonstrated the advantages of using NGA to accommodate uncertainty of hydraulic conductivity in monitoring network design, further research is needed to investigate how the methodology can be improved to further reduce the estimation errors of plume moments and how the *K*-field statistics and sampling strategies as well as GA solution parameters affect the computational accuracy and efficiency. Moreover, further study is needed to demonstrate the applicability and flexibility of the NGA methodology at large-scale field sites.

Acknowledgments

This study was supported in part by DuPont Company and the National Natural Science Foundation of China (Nos. 40472130 and 40335045). Additional support was provided by the Innovation Project (Grant No. KZCX3-SW-428) of Chinese Academy of Sciences. We are indebted to Gaisheng Liu who provided the initial code for computing the spatial moments of a contaminant plume. The authors are also grateful to the four anonymous reviewers whose constructive comments helped to improve the manuscript significantly.

References

[1] Ahlfeld DP, Mulvey JM, Pinder GF. Contaminated groundwater remediation design using simulation, optimization, and sensitivity theory. 2. Analysis of a field site. Water Resour Res 1988;24(5):443–52.

[2] Aly AH, Peralta RC. Optimal design of aquifer cleanup systems under uncertainty using a neural network and a genetic algorithm. Water Resour Res 1999;35(8):2523–32.

[3] Andricevic R. Coupled withdrawal and sampling designs for groundwater supply models. Water Resour Res 1993;29(1):5–16.

[4] Andricevic R. Evaluation of sampling in the subsurface. Water Resour Res 1996;32(4):863–74.

[5] Bear J, Sun Y. Optimization of pump-treat-inject (PTI) design for the remediation of a contaminated aquifer: multi-stage design with chance constraints. J Contam Hydrol 1998;29:225–44.

[6] Bogaert P, Russo D. Optimal spatial sampling design for the estimation of the variogram based on a squares approach. Water Resour Res 1999;35(4):1275–89.

[7] Cai X, McKinney DC, Lasdon LS. Solving nonlinear water management models using a combined genetic algorithm and linear programming approach. Adv Water Resour 2001;24:667–76.

[8] Cai X, Rosegrant MW, Ringler C. Physical and economic efficiency of water use in the river basin: implications for efficient water management. Water Resour Res 2003;39(1):1013. doi:10.1029/2001WR000748.

[9] Chien CC, Medina Jr MA, Pinder GF, Reible DR, Sleep BE, Zheng C, editors. Contaminated ground water and sediment, modeling for management and remediation. Boca Raton, Florida: Lewis Publishers; 2004. p. 274.

[10] Christakos G, Killam BR. Sampling design for classifying contamination level using annealing search algorithm. Water Resour Res 1993;29(12):4063–76.

[11] Cieniawski SE, Eheart JW, Ranjithan S. Using genetic algorithm to solve a multiobjective groundwater monitoring problem. Water Resour Res 1995;31(2):399–409.

[12] Copty NK, Findikakis AN. Quantitative estimates of the uncertainty in the evaluation of ground water remediation schemes. Ground Water 2000;38(1):29–37.

[13] Culver TB, Shoemaker CA. Dynamic optimal control for groundwater remediation with flexible management periods. Water Resour Res 1992;28(3):629–41.
[14] Deutsch CV, Journel AG. GSLIB: geostatistical software library and user's guide. 2nd ed. New York: Oxford University Press; 1998.
[15] Freeze RA, Gorelick SM. Convergence of stochastic optimization and decision analysis in the engineering design of aquifer remediation. Ground Water 1999;37(6):934–54.
[16] Freyberg DL. A natural gradient experiment on solute transport in a sand aquifer: 2. Spatial moments and the advection and dispersion of nonreactive tracers. Water Resour Res 1986;22(13): 2031–46.
[17] Goldberg DE. Genetic algorithm in search, optimization and machine learning. Reading, MA: Addison Wesley; 1989.
[18] Gopalakrishnan G, Minsker BS, Goldberg D. Optimal sampling in a noisy genetic algorithm for risk-based remediation design. In: Phelps D, Sehlke G, editors. Bridging the gap: meeting the world's water and environmental resources challenges. Proc world water and environmental resources congress. Washington DC: ASCE; 2001.
[19] Gorelick SM. A review of distributed parameter groundwater management modeling method. Water Resour Res 1983;19(2): 305–19.
[20] Harbaugh AW, Banta ER, Hill MC, McDonald MG. MODFLOW-2000, the US Geological Survey modular ground-water model–user guide to modularization concepts and the groundwater flow process. USGS Open-File Report 00-92, 2000. p. 121.
[21] Hudak PF, Loaiciga HA. A location modeling approach for groundwater monitoring network augmentation. Water Resour Res 1992;28(3):643–9.
[22] Hudak PF, Loaiciga HA. An optimization method for monitoring network design in multilayered groundwater flow system. Water Resour Res 1993;29(8):2835–45.
[23] James BR, Gorelick SM. When enough is enough: the worth of monitoring data in aquifer remediation design. Water Resour Res 1994;30(12):3499–513.
[24] Lee Y-M, Ellis JH. Comparison of algorithms for nonlinear integer optimization: application to monitoring network design. J Environ Eng 1996;122(6):524–31.
[25] Loaiciga H. An optimization approach for groundwater quality monitoring network design. Water Resour Res 1989;25(8): 1771–80.
[26] Maxwell RD, Kastenberg WE, Rubin Y. A methodology to integrate site characterization information into groundwater-driven health risk assessment. Water Resour Res 1999;35(9): 2841–55.
[27] Mayer AS, Kelley CT, Miller CT. Optimal design for problems involving flow and transport phenomena in saturated subsurface systems. Adv Water Resour 2002;25:1233–56.
[28] McDonald MG, Harbaugh AW. A modular three-dimensional finite-difference ground water flow model. USGS Techniques of Water Resources Investigations, Book 6, 1988.
[29] McKinney DC, Loucks DP. Network design for predicting groundwater contamination. Water Resour Res 1992;28(1): 133–47.
[30] McKinney DC, Lin MD. Genetic algorithm solution of groundwater management models. Water Resour Res 1994;30(6): 1897–906.
[31] Meyer PD, Valocchi AJ, Eheart JW. Monitoring network design to provide initial detection of groundwater contamination. Water Resour Res 1994;30(9):2647–59.
[32] Meyer PD, Eheart JW, Ranjithan S, Valocchi AJ. Design of groundwater monitoring networks for landfills. In: Kundzewicz ZW, editor. Proc international workshop on new uncertainty concepts in hydrology and water resources. Cambridge, 1995. p. 190–6.
[33] Miller BL. Noise, sampling, and efficient genetic algorithms. PhD dissertation, University of Ill, Urbana-Champaign, 1997.
[34] Minsker BS, Shoemaker CA. Dynamic optimal control of in situ bioremediation of ground water. J Water Resour Plann Manage 1998;124(3):149–61.
[35] Minsker BS, editor. Long-term groundwater monitoring: the state of the art. Reston, VA: ASCE/EWRI; 2003, ISBN 0-7844-0678-2.
[36] Montas HJ, Mohtar RH, Hassan AE, AlKhal FA. Heuristic space-time design of monitoring wells for contaminant plume characterization in stochastic flow fields. J Contam Hydrol 2000;43:271–301.
[37] Morgan DR, Eheart JW, Valocchi AJ. Aquifer remediation design under uncertainty using a new chance constraints programming technique. Water Resour Res 1993;29(3):551–61.
[38] Pham DT, Karaboga D. Intelligent optimization techniques: genetic algorithms, tabu search, simulated annealing and neural networks. New York: Springer-Verlag; 2000.
[39] Reed PB, Minsker B, Valocchi AJ. Cost-effective long-term groundwater monitoring design using a genetic algorithm and global mass interpolation. Water Resour Res 2000;36(12): 3731–41.
[40] Ritzel BJ, Eheart JW, Ranjithan S. Using genetic algorithms to solve a multiple-objective groundwater pollution containment problem. Water Resour Res 1994;30(5):1589–603.
[41] Rizzo DM, Dougherty DE. Design optimization for multiple management period groundwater remediation. Water Resour Res 1996;32(8):2549–61.
[42] Rouhani S, Hall TJ. Geostatistical schemes for groundwater sampling. J Hydrol 1988;103:85–120.
[43] Rouhani S. Variance reduction analysis. Water Resour Res 1985; 21(6):837–46.
[44] Sano Y, Kita H. Optimization of noisy fitness functions by means of genetic algorithms using history of search. In: Schoenauer M, Deb K, Rudolph G, Yao X, Lutton E, Merelo JJ, et al., editors. Proc 6th international conference on parallel problem solving for nature. Springer-Verlag; 2000. p. 571–81.
[45] Sen M, Stoffa PL. Global optimization methods in geophysical inversion. Elesevier Science Publishers; 1995.
[46] Smalley JB, Minsker B, Goldberg DE. Risk-based in situ bioremediation design using a noisy genetic algorithm. Water Resour Res 2000;36(10):3043–52.
[47] Storck P, Eheart JW, Valocchi AJ. A method for the optimal location of monitoring wells for detection of groundwater contamination in three-dimensional aquifers. Water Resour Res 1997;33(9):2081–8.
[48] Tiedeman C, Gorelick SM. Analysis of uncertainty in optimal groundwater contaminant capture design. Water Resour Res 1993;29(7):2139–54.
[49] Wagner BJ, Gorelick SM. Reliable aquifer remediation in the presence of spatially variable hydraulic conductivity: from data to design. Water Resour Res 1989;25(10):2211–25.
[50] Wagner BJ. Recent advances in simulation-optimization groundwater management modeling. Review of geophysics. US National Report to International Union of Geodesy and Geophysics 1991–1994, Suppl, 1995. p. 1021–8.
[51] Wagner BJ. Sampling design methods for groundwater modeling under uncertainty. Water Resour Res 1995;31(10):2581–91.
[52] Wang CG, Jamieson DG. An objective approach to regional wastewater treatment planning. Water Resour Res 2002;38(3). doi:10.1029/2000WR000062.
[53] Wang M, Zheng C. Optimal remediation policy selection under general conditions. Ground Water 1997;35(5):757–64.
[54] Wu J-F, Zheng C, Chien CC. Cost effective sampling network design for contaminant plume monitoring under general hydrogeological conditions. J Contam Hydrol 2005;77:41–65.

[55] Zheng C, Wang PP. A field demonstration of the simulation-optimization approach for remediation system design. Ground Water 2002;40(3):258–65.
[56] Zheng C, Wang PP. An integrated global and local optimization approach for remediation system design. Water Resour Res 1999; 35(1):137–48.
[57] Zheng C, Wang PP. MT3DMS: a modular three-dimensional multispecies transport model for simulation of advection, dispersion and chemical reactions of contaminants in ground water systems: Documentation and user's guide. Contract Report SERDP-99-1, US Army Engineer Research and Development Center, Vicksburg, Mississippi, 1999.